

## Defect structure and defect-defect interactions in solid solutions of $AF_2$ and $RF_3$ doped with $Gd^{3+}$ probes

H. W. den Hartog

*Solid State Physics Laboratory, University of Groningen, 1 Melkweg,  
9718 EP Groningen, The Netherlands*

(Received 30 July 1982)

In this paper we present results of an investigation of cubic  $Gd^{3+}$  ions in solid  $A_{1-x}R_xF_{2+x}$  ( $A$  is an alkaline-earth ion and  $R$  is a rare-earth ion) solutions. The values of  $x$  were chosen between 0 and 0.06 and the experimental technique used is EPR. We have observed that with increasing concentrations of the rare-earth impurities the widths of the EPR lines increase. This can be interpreted in terms of new contributions to the spin Hamiltonian originating from defect centers present in the crystal. These new contributions are second-degree crystal-field terms and can be approximated by a point-charge description of the imperfect crystal. An interesting feature of our results is that clustering does not appear to be appreciable defect clustering if we confine ourselves to the alkaline-earth elements Ca and Sr and the rare earths La, Ce, Pr, and Nd. For the heavy (small) rare-earth ions Dy, Er, and Yb the situation may be different, but these ions have not been investigated here. It appears that the defect structure of the systems  $A_{1-x}R_xF_{2+x}$  depend upon the relative sizes of the ions  $A^{2+}$ ,  $R^{3+}$ , and  $F^-$  and slight differences between the formation energies of different defects may cause drastic changes in the defect structure of the materials. This may be the reason why the trivalent Gd ions have cubic symmetry as soon as sufficient concentrations of large trivalent ions are present.

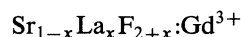
### I. INTRODUCTION

Solid solutions of the type  $A_{1-x}R_xF_{2+x}$  (where  $A$  is an alkaline-earth ion and  $R$  is a rare-earth ion) have been investigated with many experimental techniques in the recent literature.<sup>1-6</sup> It has been shown that for  $0 \leq x \leq 0.40$  the materials have the cubic crystal structure; in addition the lattice parameter deviates only slightly from that of the undoped cubic  $AF_2$  crystal. Results of ionic-thermocurrents (ITC) experiments, which have been carried out in our laboratory suggest, that in samples with large concentrations of  $R^{3+}$  ions dipolar defects govern the ionic conductivity. This conclusion does not hold for all systems studied in our laboratory. Preliminary experimental results on  $Sr_{1-x}Dy_xF_{2+x}$ ,  $Sr_{1-x}Er_xF_{2+x}$ , and  $Sr_{1-x}Yb_xF_{2+x}$  indicate that these materials behave differently because of extensive clustering. The crystals studied in this paper, however, do not show extensive clustering.

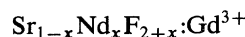
In this paper we shall investigate the defect structure of heavily doped  $A_{1-x}R_xF_{2+x}$  single crystals, which contain very small amounts of  $Gd^{3+}$  probes. The latter impurity is a very suitable one to study with EPR. The magnetic energy levels of the  $4f^7$  ground state of  $Gd^{3+}$  are very sensitive to variations

in the crystal-field interactions. In addition this probe can be employed for experiments in a wide temperature range. The experimental results obtained from the present study provide us with information concerning eventual clustering. Also the width of the EPR lines can be used to describe the defect structure of heavily doped crystals. As mentioned above, the fine structure of the  $Gd^{3+}$  ion is quite sensitive to the interaction with the surrounding crystal lattice. Distant dipoles produce an electrostatic crystal-field potential at the  $Gd^{3+}$  impurity position. Because the relative positions of the  $R^{3+}$  ions and the  $Gd^{3+}$  probes show an approximately statistical behavior the fine lines are scattered statistically about their central (cubic) position and we expect that the width of the observed lines will increase with an increasing concentration of  $R^{3+}$  ions in the lattice surrounding the  $Gd^{3+}$  probe.

We have analyzed our results on crystals of the types



and



on the basis of a statistical distribution of La and

Nd ions and taking into account electrostatic interactions between the  $Gd^{3+}$  probes and the  $R^{3+}-F_i^-$  dipoles. It is concluded that both the behavior of the linewidth as a function of the  $R$  concentration and the absolute values of the linewidth can be reproduced reasonably well by our model. An interesting feature of our results is that up to very high La or Nd concentrations the Gd impurities are located at cubic positions. The EPR lines associated with low-symmetry  $Gd^{3+}$  ions are absent or very weak, implying that this impurity does not participate in the clustering process.

## II. EXPERIMENTAL PROCEDURES

The materials used for this investigation were prepared with a Bridgman crystal-growing setup. The furnace is powered by a high-frequency generator operating at 800 kHz; the maximum power available is 25 kW. The  $CaF_2$  and  $SrF_2$  together with the impurities  $LaF_3$  and  $NdF_3$  and a small amount of  $GdF_3$  are heated in high-purity carbon crucibles. In one run we can grow seven crystals at the same time; in this way the different samples are grown under the same conditions. The resulting single crystals have a diameter of 8 mm; the length is about 30 mm. The  $Gd^{3+}$  probes are added in the same way as La and Nd; in order to obtain a sufficiently intense EPR signal the nominal concentration of the  $Gd^{3+}$  impurities was chosen between 10 and 100 ppm.

The EPR experiments have been carried out with a Varian X-band EPR spectrometer. The observations have been made at room temperature. For the determination of the linewidth we have aligned the sample with one of the  $\langle 100 \rangle$  axes along the magnetic field direction. This has several advantages: We have to orient the sample such that the fine splitting reaches its maximum value; in addition the system of principal axes is  $[100]$ ,  $[010]$ , and  $[001]$ , which makes the theoretical analysis of the broadening results relatively simple. The different samples were oriented with  $[001]$  along the magnetic field direction. Subsequently, the width of all transitions  $S_z \leftrightarrow S_z - 1$  are measured. For the width of the lines we take the distance (in Gauss) between the two extreme values of the first-derivative spectrum, which is for a Gaussian peak equal to  $1/(2 \ln 2)^{1/2}$  times the width at half height. The observed linewidths are compared with those calculated theoretically with the method outlined in Sec. IV.

## III. EXPERIMENTAL RESULTS

$CaF_2$  and  $SrF_2$  crystals doped with small amounts of  $Gd^{3+}$  show an EPR signal which has been as-

cribed to tetragonal and trigonal complexes consisting of one  $Gd^{3+}$  ion and an interstitial  $F^-$  ion. The structure of these complexes is well known and has been studied by means of different techniques.<sup>7-9</sup> If the crystals are doped with  $Gd^{3+}$  probes together with variable amounts of  $La^{3+}$  impurities, one finds that the intensity of the signals due to axial complexes is reduced; instead a spectrum showing cubic symmetry is observed. In our materials the addition of only a few hundred ppm of  $LaF_3$  is sufficient to suppress the axial signals completely. In these samples we only observe a cubic signal.

In Fig. 1 we show the EPR signal of a  $SrF_2$  crystal doped with  $GdF_3$  and 0.1 mol %  $LaF_3$ . The magnetic field direction is chosen along  $[100]$ . For some of the EPR lines we observed that the superhyperfine structure is resolved partly, implying that we are dealing with high-quality and very slightly doped materials. If we add more  $LaF_3$  we observe a broadening of the EPR lines; the magnitude of the broadening effect depends upon the concentration of the La impurities. This is demonstrated in Fig. 2 where we have given two more EPR spectra associated with cubic  $Gd^{3+}$  impurities in solid solutions  $Sr_{1-x}La_xF_{2+x}$ ; the values of  $x$  are chosen in the interval 0–0.06.

Similar broadening effects have been observed for some other cubic solid solutions of the type  $A_{1-x}R_xF_{2+x}$  ( $A = Ca$  or  $Sr$  and  $R$  is a rare-earth ion). In some cases we have observed apart from the lines associated with cubic  $Gd^{3+}$  additional peaks which are probably due to centers with point symmetry lower than the cubic one. An example has been given in Fig. 3; especially the sample doped with 0.15 mol %  $LaF_3$  shows many extra lines. These extra lines have not been investigated in detail, but it is assumed that they are due to complexes

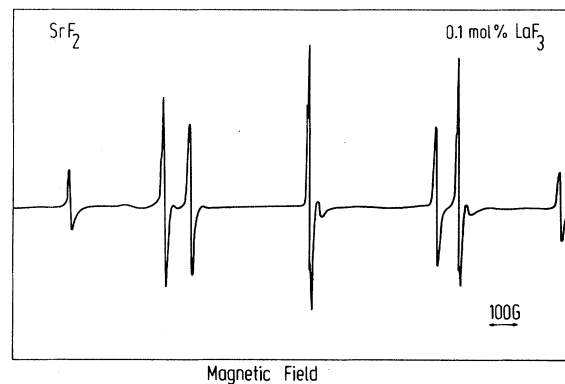


FIG. 1. EPR spectrum of a  $SrF_2$  crystal containing 0.1 mol %  $LaF_3$  and a small concentration of  $Gd^{3+}$  probes. The measurement was carried out at room temperature and the magnetic field was aligned along the crystallographic  $[100]$  axis.

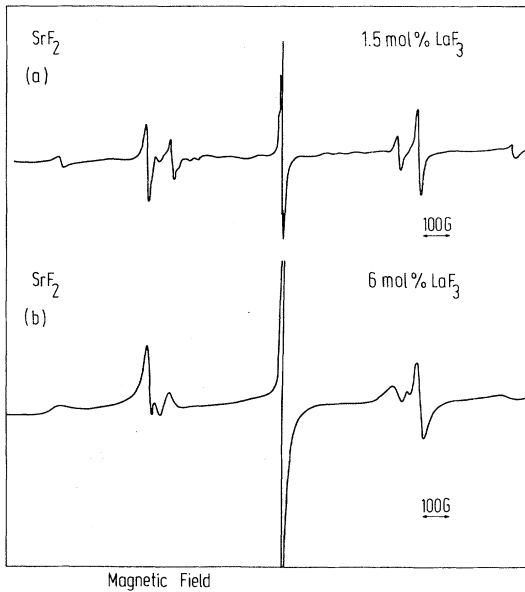


FIG. 2. (a) EPR spectrum of  $\text{Sr}_{0.985}\text{La}_{0.015}\text{F}_{2.015}:\text{Gd}^{3+}$  taken at room temperature with  $\vec{H}_0 \parallel [100]$ . (b) EPR spectrum of  $\text{Sr}_{0.94}\text{La}_{2.06}:\text{Gd}^{3+}$  taken at room temperature with  $\vec{H}_0 \parallel [100]$ .

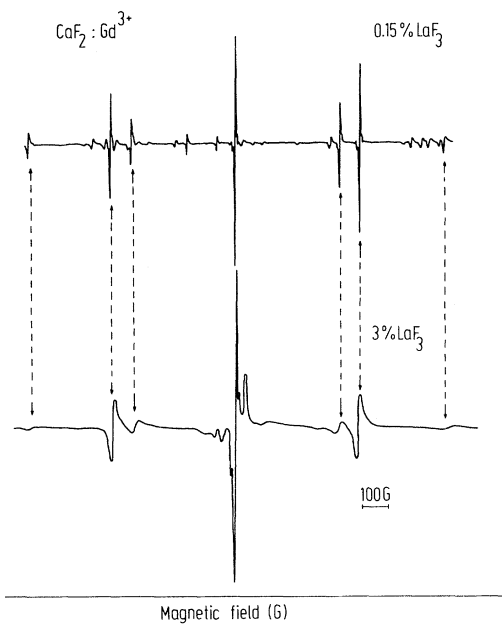


FIG. 3. (a) EPR spectrum of a  $\text{CaF}_2$  crystal doped with 0.15 mol %  $\text{LaF}_3$  and a small concentration of  $\text{Gd}^{3+}$  probes. The measurement was carried out at room temperature and the magnetic field was aligned along the crystallographic  $[100]$  axis. (b) EPR spectrum of  $\text{Ca}_{0.97}\text{La}_{0.03}\text{F}_{2.03}:\text{Gd}^{3+}$  taken at room temperature with  $\vec{H}_0 \parallel [100]$ .

containing one  $\text{Gd}^{3+}$  ion and one or more La impurities. Comparing the upper and lower trace in Fig. 3 we see that adding more and more  $\text{LaF}_3$  does not lead to an increase of the intensity of the lines already present in the upper spectrum. Therefore, if clustering plays a role it is different at low and high La concentrations. From earlier ITC experiments on rare-earth-doped  $\text{CaF}_2$  crystals we have concluded that there is clustering in these materials at relatively low concentrations.<sup>9</sup> From Fig. 3 we see that cubic  $\text{Gd}^{3+}$  is still dominant for La concentrations as high as 3 mol %.

An interesting feature of the results presented in both Figs. 2 and 3 is that the broadening effect on the transition  $S_z \leftrightarrow S_z + 1$  increases considerably with the quantum number  $S_z$ . The broadening of the transition  $S_z = -\frac{1}{2} \leftrightarrow \frac{1}{2}$  is small, but it is large for the transitions  $-\frac{7}{2} \leftrightarrow -\frac{5}{2}$  and  $\frac{5}{2} \leftrightarrow \frac{7}{2}$ . In Fig. 4 we have plotted the broadening effect of the La impurities in  $\text{CaF}_2:\text{Gd}^{3+}$  on the various fine transitions as a function of the La concentration. An interesting feature of the results is that for La concentrations up to 6 mol % the width of the EPR lines depends linearly upon the concentration. Another im-

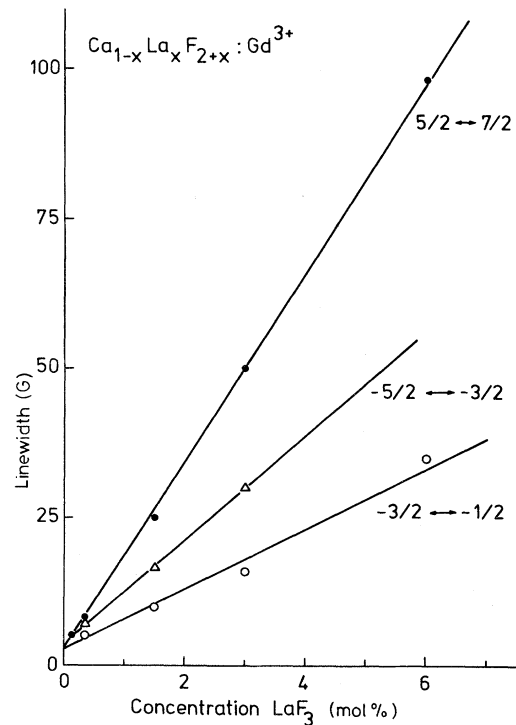


FIG. 4. Behavior of the ESR linewidths ( $p$ - $p$  values) of some  $S_z \leftrightarrow S_z + 1$  transitions in  $\text{Ca}_{1-x}\text{La}_x\text{F}_{2+x}:\text{Gd}^{3+}$  as a function of  $x$ . The different  $S_z \leftrightarrow S_z + 1$  transitions have been indicated. The slopes of the lines obey the following relation 1:2:3.

portant feature is that the slopes for the transitions  $-\frac{7}{2} \leftrightarrow -\frac{5}{2}$ ,  $-\frac{5}{2} \leftrightarrow -\frac{3}{2}$ ,  $-\frac{3}{2} \leftrightarrow -\frac{1}{2}$ ,  $\frac{1}{2} \leftrightarrow \frac{3}{2}$ ,  $\frac{3}{2} \leftrightarrow \frac{5}{2}$ , and  $\frac{5}{2} \leftrightarrow \frac{7}{2}$  have the ratio 3:2:1:1:2:3, while the broadening of the transition  $-\frac{1}{2} \leftrightarrow \frac{1}{2}$  is very small.

The above-mentioned effects have also been observed for the systems  $\text{Sr}_{1-x}\text{La}_x\text{F}_{2+x}$  and  $\text{Sr}_{1-x}\text{Nd}_x\text{F}_{2+x}$  in which Gd probes are present. In crystals of the type  $\text{Sr}_{1-x}\text{La}_x\text{F}_{2+x}$  the broadening effect is not an exact linear function of the La concentration (Fig. 5). It increases more rapidly with the concentration. Probably the coagulation of defects in  $\text{SrF}_2$  is less important than in  $\text{CaF}_2$ . Because the effect of clusters on the cubic  $\text{Gd}^{3+}$  EPR lines will be small, the broadening of the lines in  $\text{SrF}_2$  will be larger than in  $\text{CaF}_2$ . In ITC we have observed that clustering of dipolar defects is stronger in  $\text{Ca}_{1-x}\text{La}_x\text{F}_{2-x}$  than in  $\text{Sr}_{1-x}\text{La}_x\text{F}_{2+x}$ . Especially for  $\text{Ca}_{1-x}\text{La}_x\text{F}_{2+x}$  we have observed that quenching of the samples from 1150–1200°C leads to an appreciable increase of the ITC peaks associated with simple  $\text{La}^{3+}\text{-F}_i^-$  dipolar defects. This observation is in agreement with the EPR results obtained during this investigation showing that clustering in  $\text{CaF}_2$  is more extensive than in  $\text{SrF}_2$ .

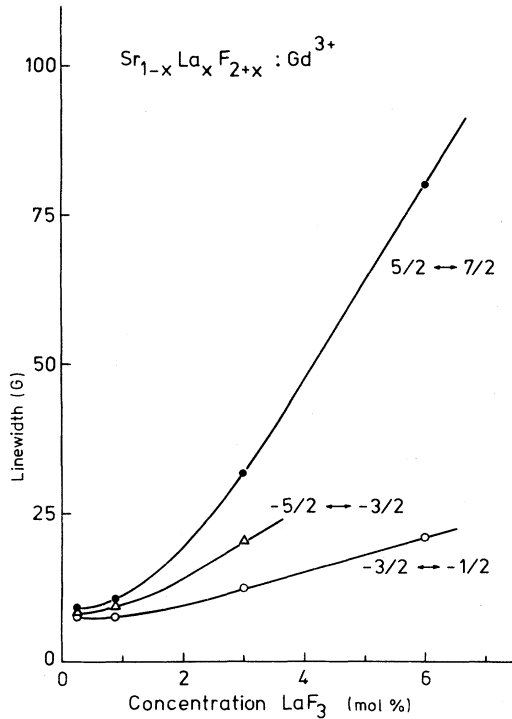


FIG. 5. Behavior of the ESR linewidths ( $p$ - $p$  values) of some of the  $S_z \leftrightarrow S_z + 1$  transitions in  $\text{Sr}_{1-x}\text{La}_x\text{F}_{2+x}:\text{Gd}^{3+}$  as a function of  $x$ . The different  $S_z \leftrightarrow S_z + 1$  transitions have been indicated.

#### IV. THEORY

In ionic crystals the crystal-field interaction between the  $\text{Gd}^{3+}$   $4f^7$ -electron system and the surrounding particles is mainly determined by electrostatic interactions. This has been shown by a series of papers by Bijvank and den Hartog.<sup>10-13</sup> These authors have investigated in detail the crystal-field interaction parameters  $B_2^0$  and  $B_2^2$  and the parameter  $c_1^0$  describing the first-order Stark splitting of  $\text{Gd}^{3+}\text{-M}^+$  complexes in alkaline-earth fluorides.

The spin Hamiltonian associated with cubic  $\text{Gd}^{3+}$  impurities in alkaline-earth fluorides can be written as (if the principal axes are chosen along one of the  $\langle 100 \rangle$  directions)

$$\mathcal{H}_c = g\mu_B \vec{H} \cdot \vec{S} + B_4 O_4 + B_6 O_6 + \sum_{i=1}^6 \vec{I}_i \vec{a}_i \vec{S}, \quad (1)$$

where the first term is the Zeeman interaction; the second and third terms are due to the fourth- and sixth-degree crystal-field interaction. The fourth term describes the superhyperfine interaction between the  $\text{Gd}^{3+}$  electron-spin system and the nuclear spins of the nearest  $\text{F}^-$  neighbors.

If in the vicinity of the  $\text{Gd}^{3+}$  impurity there is another trivalent impurity, an interstitial fluoride ion, or a charge-compensation center (electrical dipole) the crystal field felt by the  $\text{Gd}^{3+}$  ion is slightly different from the cubic one. Because the defects are distributed more or less statistically over the lattice positions available, the additional crystal-field terms to be added also vary statistically.

The Coulomb contribution of an excess charge  $q$  located at  $\vec{R}$  is equal to (only the second-degree term is taken into account)

$$\begin{aligned} V_2(q, \vec{R}, \vec{r}) = & \frac{q}{16\pi\epsilon_0} \frac{3Z^2 - R^2}{R^5} (3z^2 - r^2) \\ & + \frac{3q}{16\pi\epsilon_0} \frac{X^2 - Y^2}{R^5} (x^2 - y^2) \\ & + \frac{3q}{16\pi\epsilon_0} \frac{(2XY)}{R^5} (2xy). \end{aligned} \quad (2)$$

The excess charge can be either a trivalent impurity or an interstitial fluoride ion. For the description of the broadening effect we have only taken into account second-degree interactions, because of the observed ratio of the contributions to the widths of the various  $S_z \leftrightarrow S_z - 1$  transitions.

In order to describe the broadening of the EPR lines theoretically, we construct a model material consisting of spheres in each of which we have one  $\text{La}^{3+}\text{-F}_i^-$  dipole; if  $n$  is the number of  $\text{Sr}^{2+}$  sites within the sphere,  $1/n$  is the concentration of  $\text{La}^{3+}$  ions in the crystal. It is assumed that the probabili-

ty of finding the impurity at any of the available positions within the sphere is the same; i.e., the distribution of  $\text{La}^{3+}\text{-F}_i^-$  dipoles is statistical. In our calculations we consider the contribution from *all* possible configurations of one defect pair inside the sphere with a cubic  $\text{Gd}^{3+}$  ion at the center.

We note that eventual clustering will give rise to deviations from our theoretical model. Some of the clusters (i.e., those containing, apart from one or more  $\text{La}^{3+}\text{-F}_i^-$  pairs, one  $\text{Gd}^{3+}\text{-F}_i^-$  pair) should be observable with EPR, if they are present in sufficient concentrations, because of the very specific crystal-field parameters of these clusters. In most of the samples investigated in this paper we did not observe any of these clusters; in the samples showing extra EPR lines, the signals were weak indicating that clustering does not play an important role.

For our EPR experiments we take  $\vec{H}_0 \parallel [100]$ ; in this situation the broadening of the EPR lines can be described by the first term of Eq. (2). The second and third term of the second-degree crystal-field Hamiltonian only contribute in second and higher order. Thus to explain our results we can use the following relation:

$$B_2^0 = 10.2 \times 10^{18} \frac{e}{16\pi\epsilon_0} \times \left[ \frac{3Z_{\text{La}}^2 - R_{\text{La}}^2}{R_{\text{La}}^5} - \frac{3Z_{\text{Fi}}^2 - R_{\text{Fi}}^2}{R_{\text{Fi}}^5} \right]. \quad (3)$$

Because of the presence of the dielectric between the central Gd ion and the perturbing dipoles we have to multiply the crystal-field parameter by a factor (this factor can be calculated using the dielectric theory outlined in Ref. 15)

$$f = \frac{3}{2\epsilon + 1}, \quad (4)$$

which is equal to 0.2053, 0.2152, and 0.1908 for  $\text{CaF}_2$ ,  $\text{SrF}_2$ , and  $\text{BaF}_2$ , respectively. Using the results of Eqs. (3) and (4) we can now calculate the histograms showing the distributions of the  $B_2^0$  values associated with different concentrations of  $\text{La}\text{-F}_i$  dipoles. Some examples of our results have been presented in Fig. 6; we have fitted the histogram to a Gaussian distribution and calculated the width at half height  $p$ . A survey of the calculated broadening effect as a function of the concentration has been plotted in Fig. 7. One observes that the width is not a linear function of the concentration. The distribution of  $B_2^0$  values as calculated here leads to a distribution of peak positions of the various  $S_z \leftrightarrow S_z - 1$  transitions measured. The shifts of the lines associated with a certain value of  $B_2^0$  depend upon the transition considered. Therefore, the perturbation due to dipoles surrounding the  $\text{Gd}^{3+}$

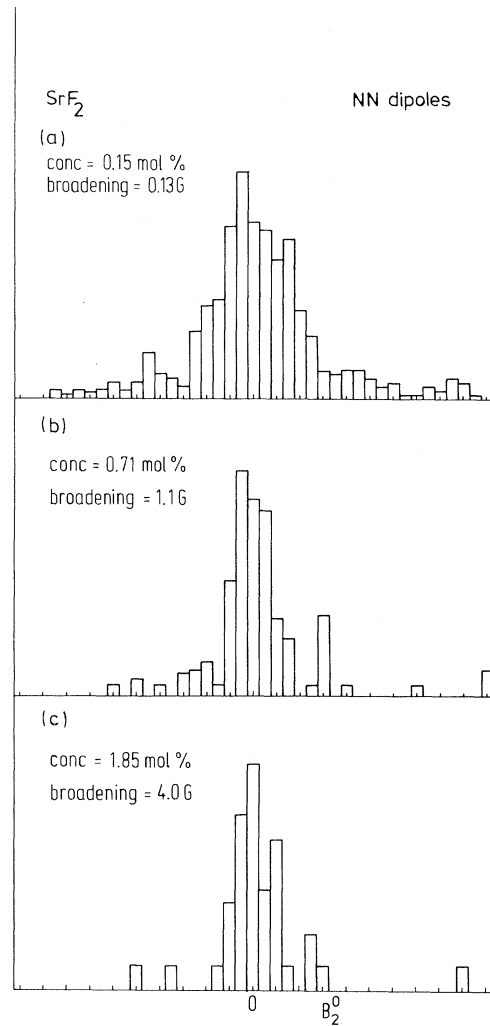


FIG. 6. Theoretically calculated histograms showing the distributions of  $B_2^0$  values for NN-type  $\text{La}^{3+}\text{-F}_i^-$  concentrations of 0.15, 0.71, and 1.85 mol %. The width of the blocks in the histograms are different; for (a), (b), and (c) the widths of the blocks are 0.015, 0.25, and 1 G, respectively. The values of the broadening parameter indicated are equal to the width of the  $B_2^0$  distributions at half height.

impurity will lead to different broadening effects for different  $S_z \leftrightarrow S_z - 1$  transitions. If the broadening is governed by second-degree perturbations, as we assume to be the case in the systems studied in this investigation, it leads to contributions to the linewidth of the  $S_z = -\frac{5}{2} \rightarrow -\frac{7}{2}$ ,  $-\frac{3}{2} \rightarrow -\frac{5}{2}$ , and  $-\frac{1}{2} \rightarrow -\frac{3}{2}$ .  $\frac{1}{2} \rightarrow -\frac{1}{2}$ ,  $\frac{3}{2} \rightarrow \frac{1}{2}$ ,  $\frac{5}{2} \rightarrow \frac{3}{2}$ , and  $\frac{7}{2} \rightarrow \frac{5}{2}$  peaks have the ratio 3:2:1:0:1:2:3. If, on the other hand, there is an appreciable contribution due to fourth-degree or sixth-degree crystal-field terms this ratio is not observed.

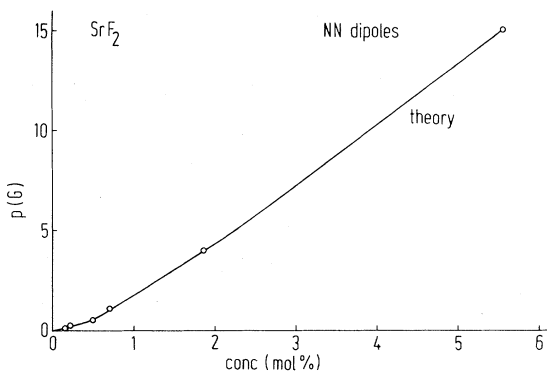


FIG. 7. Theoretically calculated broadening parameter  $p$  (see also Fig. 6) for the system  $\text{Sr}_{1-x}\text{La}_x\text{F}_{2+x}:\text{Gd}$  assuming that the NN-type  $\text{La}^{3+}-\text{F}_i^-$  dipoles in  $\text{SrF}_2$  are distributed statistically over the Sr lattice positions and assuming that each of these impurities is connected with a nearest-neighbor interstitial fluoride ion (see also Fig. 8).

We note that in our calculations we have used the undistorted point-ion model (UPIM) although we know that the dipole strength calculated in this way is too large. Aalbers and den Hartog<sup>7</sup> have found that for  $\text{Gd}^{3+}-\text{F}_i^-$  dipoles of the nearest-neighbor (NN) type in  $\text{SrF}_2$  are a factor of 0.79 smaller than the UPIM value. Wapenaar has calculated for  $\text{La}^{3+}-\text{F}_i^-$  dipoles a correction factor of 0.70.<sup>8</sup> It is now reasonable to apply this correction factor to the observed theoretical values for  $B_2^0$  before we compare the experimental and theoretical results for the  $\frac{7}{2} \leftrightarrow \frac{5}{2}$  transition in Fig. 8.

## V. DISCUSSION

Our experimental results show that solid solutions of the type  $\text{Ca}_{1-x}\text{R}_x\text{F}_{2+x}$  and  $\text{Sr}_{1-x}\text{R}_x\text{F}_{2+x}$  have the cubic structure for  $x \leq 0.06$ . In addition, the fact that the magnitude of the cubic crystal-field-splitting parameter is not affected by the presence of the trivalent rare-earth impurities indicates that the lattice parameter is approximately constant for  $0 \leq x \leq 0.06$ . In general, the fluorite-type alkaline-earth fluorides form solid solutions for  $R$  concentrations up to 30–40 mol%. This implies also that  $\text{RF}_3$  molecules are well accommodated in the fluorite-crystal structure.

There are several possible ways in which we can introduce trivalent impurities in the fluorite lattice; two of them have been represented schematically in Fig. 9. These centers are local charge compensators. Another possibility is the nonlocal charge compensation. In that case we are dealing with an  $R$  impurity with cubic point symmetry. The situations

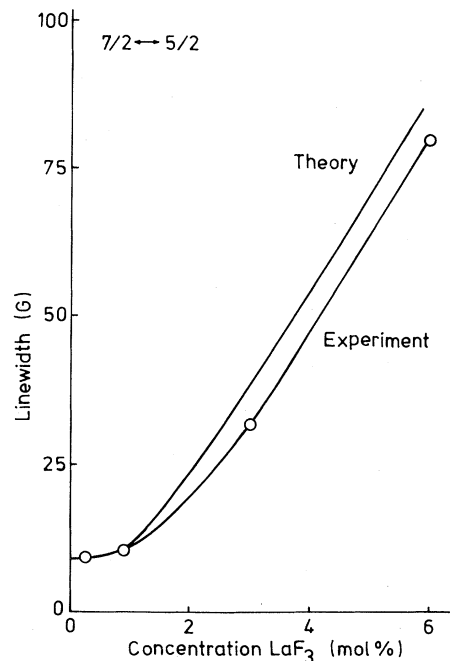


FIG. 8. Comparison of the calculated linewidth, using the theoretical model described in Sec. IV, and the experimentally observed one for the  $\frac{7}{2} \leftrightarrow \frac{5}{2}$  transition of cubic  $\text{Gd}^{3+}$  with  $\vec{H}_0 || [100]$ .

described above are expected to occur at low  $R$  concentrations. At high concentrations clusters may be formed, especially if association of defects is energetically favorable.

In an earlier paper we have studied the defect structure of  $\text{SrF}_2$  crystals doped with different lanthanide ions.<sup>8</sup> The conclusion that can be drawn

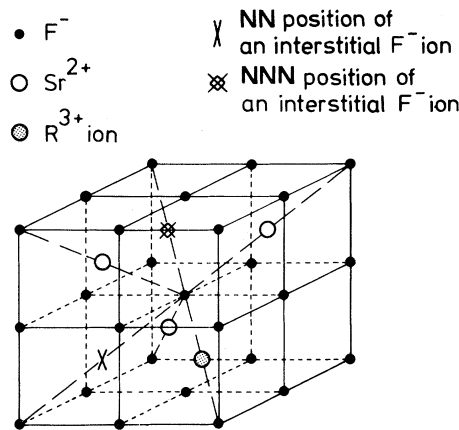


FIG. 9. Schematic representation of the  $\text{SrF}_2$  lattice containing a rare-earth ion associated with a nearest-neighbor or a next-nearest-neighbor interstitial fluoride ion.

from the results of these investigations is that the defects present in  $\text{SrF}_2$  depend upon the radius of the trivalent impurity. The large ones (e.g., La, Ce, and Pr) are present predominantly as tetragonal (NN) dipoles; the small ones (Yb and Lu) form trigonal next-nearest-neighbor (NNN) dipoles. We expect that just as for the formation of simple dipoles the ionic radius of the impurity is of importance for clustering also. Particularly, the difference between the radii of the host-lattice ion and the impurity should be considered. We note that this point limits the conclusiveness of the EPR results on  $A_{1-x}\text{La}_x\text{F}_{2+x}:\text{Gd}$ .

Firstly, if in the neighborhood of the cubic  $\text{Gd}^{3+}$  probes there are clusters consisting of two or more  $\text{La}^{3+}\text{-F}_i^-$  dipole pairs the effect of the defects on the linewidth of the  $S_z \leftrightarrow S_z + 1$  transition will be reduced drastically as compared to that of a system with single  $\text{La}^{3+}\text{-F}_i^-$  dipole pairs only. This is due to the fact that in a crystal containing coagulated defects the average distance between the  $\text{Gd}^{3+}$  probes and the perturbing defects will be larger than in a crystal with single  $\text{La}^{3+}\text{-F}_i^-$  dipole pairs only. Secondly, it is expected that clusters consisting of two or more  $\text{La}^{3+}\text{-F}_i^-$  pairs cause significant electrostatic quadrupole and higher multipole fields, while the dipole fields are less important. The crystal field felt by the  $\text{Gd}^{3+}$  probes due to clusters, therefore, in general fall off more rapidly than for pure dipoles. From the observed agreement between theory and experiment (see Fig. 8) we conclude that clustering of  $\text{La}^{3+}\text{-F}_i^-$  dipoles is unimportant. In addition we found from our experimental results that  $\text{Gd}^{3+}$  ions do not participate in an eventual clustering process either. We have observed only very weak EPR lines, which can be ascribed to low

symmetry  $\text{Gd}^{3+}$  ions. This suggests that the broadening of the EPR lines of the cubic  $\text{Gd}^{3+}$  probes due to the electrostatic interactions with distant clusters containing both  $\text{Gd}^{3+}$  and  $\text{La}^{3+}$  is negligibly small. From a comparison of our experimental and theoretical results obtained for the systems  $\text{Sr}_{1-x}\text{La}_x\text{F}_{2+x}$  (see Fig. 8) and  $\text{Sr}_{1-x}\text{Nd}_x\text{F}_{2+x}$  we draw the conclusion that for the first ions in the series of lanthanides clustering is unimportant.

Another feature of our experimental results, i.e., the fact that in samples doped with both  $\text{Gd}^{3+}$  and  $\text{La}^{3+}$  one observes predominantly cubic  $\text{Gd}^{3+}$ , needs an explanation. It has been suggested by some authors<sup>2,14-16</sup> that clustering of defects is the origin of this phenomenon, which has been observed in both  $\text{CaF}_2$  and  $\text{SrF}_2$ . It has been proposed that lanthanum impurities may trap more than one interstitial fluoride ion each. We note, however, that there is an alternative explanation for the observation that the number of axial  $\text{Gd}^{3+}$  impurities is reduced drastically if  $\text{LaF}_3$  is added. The energy of dissociation of axial complexes consisting of a trivalent impurity and an interstitial fluoride ion is a few tenths of an electron volt. From an earlier investigation on tetragonal and trigonal complexes we know that the energy of formation of these complexes is a function of the radius of the trivalent impurity.

We assume that the energy of formation of a tetragonal La-F complex is larger than that of a Gd-F complex. At finite temperatures a fraction of the interstitial fluoride ions has dissociated from the trivalent impurity ions. With increasing La concentrations the number of nonlocally compensated  $\text{Gd}^{3+}$  impurities will increase. This behavior agrees qualitatively with what has been observed experimentally.

- <sup>1</sup>E. L. Kitts Jr. and J. H. Crawford, Phys. Rev. B 9, 5264 (1974).  
<sup>2</sup>D. R. Tallant, D. S. More, and J. C. Wright, J. Chem. Phys. 67, 2898 (1977).  
<sup>3</sup>P. D. Southgate, J. Chem. Phys. Solids 17, 1623 (1966).  
<sup>4</sup>R. J. Booth, M. R. Mustafa, and B. R. McGarvey, Phys. Rev. B 17, 4150 (1978).  
<sup>5</sup>A. K. Cheetham, B. E. F. Fender, and M. J. Cooper, J. Phys. C 4, 3107 (1971).  
<sup>6</sup>D. van der Marel and H. W. den Hartog, Phys. Rev. B 25, 11 (1982).  
<sup>7</sup>A. B. Aalbers and H. W. den Hartog, Phys. Rev. B 19, 2163 (1979).  
<sup>8</sup>K. E. D. Wapenaar, Ph.D thesis, University of Utrecht, 1981 (unpublished).  
<sup>9</sup>B. P. M. Lenting, J. A. J. Numan, E. J. Bijvank, and H.

- W. den Hartog, Phys. Rev. B 16, 2953 (1977).  
<sup>10</sup>Z. C. Nauta-Leeffers and H. W. den Hartog, Phys. Rev. B 19, 4162 (1979).  
<sup>11</sup>E. J. Bijvank and H. W. den Hartog, Phys. Rev. B 12, 4646 (1975).  
<sup>12</sup>E. J. Bijvank, H. W. den Hartog, and J. Andriessen, Phys. Rev. B 16, 1008 (1977).  
<sup>13</sup>E. J. Bijvank and H. W. den Hartog, Phys. Rev. B 22, 4121 (1980).  
<sup>14</sup>E. J. Bijvank and H. W. den Hartog, Phys. Rev. B 22, 4133 (1980).  
<sup>15</sup>H. Fröhlich, *Theory of Dielectrics* (Clarendon, Oxford, 1957); C. J. F. Böttcher, *Theory of Electric Polarization* (Elsevier, Amsterdam, 1973), Vol. 1.  
<sup>16</sup>J. H. Crawford and G. E. Matthews, Semicond. Insul. 2, 213 (1977).